

Modelling Crack Propagation in AGR Graphite Bricks in Code_Aster Using the eXtended Finite Element Method

P. Martinuzzi¹ and L. Pellet¹

¹ EDF Energy R&D UK Centre, seconded at the Modelling and Simulation Centre, University of Manchester. George Begg Building, Manchester M13 9PL, U.K.

philippe.martinuzzi@eleves.enpc.fr, laure.pellet@edf.fr

ABSTRACT. *Demonstrating the structural capacity of graphite cores of Advanced Gas-cooled Reactors (AGR) is essential for their operation. The Plant Life Extension programme of EDF Energy Nuclear Generation aims at supporting the lifetime extension of power plants. In that scope, the understanding and evaluation of both crack initiation and crack propagation in the particular case of graphite bricks is a key point. The present paper focuses on crack propagation using the eXtended Finite Element Method (X-FEM) in Code_Aster. A first study aims at determining the capabilities and the limits of this method. Mesh dependency, and the accuracy of the calculation of the Stress Intensity Factors (SIF) and the strain energy release rate, which have a major role in crack propagation, are studied. Then, propagation criteria adapted to quasi-static brittle cracking are tested. Three gradually complex test cases are identified, studied, and compared with experimental results made on an un-irradiated graphite brick in order to validate the propagation criteria and their robustness. The influence of both the propagation criteria and the initial crack shape on the crack path is analysed.*

INTRODUCTION

AGR Graphite moderator bricks experience constantly evolving stresses and deformations due to heterogeneous irradiation damage, temperature and radiolytic oxidation. The mechanical properties of graphite are also significantly changing during its lifetime (e.g. the Young's Modulus can vary from 10 to 30 GPa). Though these modifications are studied [1], the numerical analyses presented in this paper are made on un-irradiated bricks. Graphite is considered here as a homogeneous linear elastic material with a Young's Modulus and a Poisson's ratio of respectively 10 GPa and 0.2.

This paper presents results obtained with Code_Aster using the eXtended Finite Element Method (X-FEM). This method allows crack propagation through the element, and thus prevents from remeshing the part. It is based on the partition of unity [2]. Its description, as well as the level set representation of the crack and the enrichment of the elements, is given by Belytschko et al. in [3]. This paper doesn't aim at focusing on the accuracy of crack representation with X-FEM but on crack propagation criteria for brittle cracking and their implications on the obtained crack path. Crack paths obtained

with several loadings applied to graphite bricks are compared with experimental results. Their accuracy is evaluated by analysing the evolution of the values of the Stress Intensity Factors (SIF) and of the strain energy release rate (G) with crack propagation.

LINEAR ELASTIC FRACTURE MECHANICS

Stress Intensity Factors and Strain Energy Release rate

Crack propagation criteria rely on linear elastic fracture mechanics. The stress state around the crack tip is determined via the calculation of the stress intensity factors (K_I , K_{II} and K_{III}). They are defined in Eqs 1, 2 and 3 (r is the radius, and the σ_{ij} are the stress components in the Cauchy stress tensor).

$$\text{Mode I : opening mode} \quad K_I = \lim_{r \rightarrow 0} \sqrt{2\pi r} \sigma_{yy}(r,0) \quad (1)$$

$$\text{Mode II : sliding mode} \quad K_{II} = \lim_{r \rightarrow 0} \sqrt{2\pi r} \sigma_{yx}(r,0) \quad (2)$$

$$\text{Mode III : tearing mode} \quad K_{III} = \lim_{r \rightarrow 0} \sqrt{2\pi r} \sigma_{yz}(r,0) \quad (3)$$

The contribution of the third mode to crack propagation is not well understood. Moreover, the crack should propagate in order to maximize the opening mode [4], especially for brittle materials and when there is no contact between the crack surfaces. Thus, one physical argument to validate the crack path obtained numerically is to check that the K_{II}/K_I ratio is and remains low (in the rest of the paper, we will refer to this as the Mode I dominating propagation).

The energy dissipated per unit of surface during fracture is determined via the calculation of the strain energy release rate G . Its definition is given in Eq. 4 (U is the potential energy available for crack propagation and A is the crack area).

$$G = -\frac{\partial U}{\partial A} \quad (4)$$

For the 3D cases studied here, the values of G should remain as constantly distributed as possible along the crack front [5]. Thus, one physical argument to validate the numerical crack path is to check that the dispersion of the values of G in the crack front is low (in the rest of the paper, we will refer to this as the iso- G propagation). For this study, the evolution of the relative standard deviation (standard deviation divided by the average value) of the values of G calculated on the points of the crack front is analysed.

Numerical Calculation

One of the most precise ways to calculate both the SIF and G is to use the G -Theta method [6], which basically evaluates the values by introducing a theta field that represents the imaginary propagation of the crack.

The SIF and G are calculated on an area limited by an integration contour. Theoretically, results are independent of this integration contour, but for numerical reasons, it is recommended to define it in accordance with the mesh size. In order to evaluate mesh dependency on crack path, a plain strain 2D model that generates mixed mode was considered and meshed with several meshes with different element sizes. The results showed that provided that the mesh was fine enough to be able to introduce a sufficiently small initial crack and a small length of propagation, crack path is similar for each mesh.

However, in 3D, for numerical reasons, errors in crack path can appear due to a misvaluation of the SIF and G. Indeed, the values are well evaluated only when the integration contour remains entirely in the material. When it is partly defined on both the material and the outside, the calculation is wrong. Thus, in 3D, with emerging cracks, values are systematically misvaluated in the extremities of the crack front. This misvaluation is quite concerning because the values of the SIF and G are smoothed (they are approximated with Legendre Polynomials). Thus, the calculation errors in the extremities may in certain cases propagate on other points of the crack front.

CRACK PROPAGATION CRITERIA

Direction of Propagation Criteria

In this paper we focus on two widely used criteria for the direction of propagation: the maximum hoop stress criterion and the maximum strain energy release rate criterion. They both are local criteria deduced from the values of the first two SIF. They are presented in [7].

The maximum hoop stress criterion states that the crack propagates in the direction where the hoop stress, $\sigma_{\theta\theta}$, is maximal. The hoop stress around the crack tip can be deduced from the values of the first two SIF. This directly leads to the angle of propagation θ given in Eq. 5.

$$\theta = \cos^{-1} \left(\frac{3K_{II}^2 + \sqrt{K_I^4 + 8K_I^2 K_{II}^2}}{K_I^2 + 9K_{II}^2} \right) = 2 \tan^{-1} \left(\frac{1}{4} \left(\frac{K_I}{K_{II}} - \text{sign}(K_{II}) \sqrt{\left(\frac{K_I}{K_{II}} \right)^2 + 8} \right) \right) \quad (5)$$

The maximum strain energy release rate criterion relies on a theory that deduces the values of the SIF for the next step of propagation (depending on the angle of propagation θ) from the values of the SIF for the current step. An imaginary value of G is then calculated (depending on θ) and the direction chosen is the one that maximizes $G(\theta)$. This is a matrix problem that requires more computational time.

Theoretically, both criteria give very close results, especially when the opening mode is dominating, but the maximum hoop stress criterion is more convenient to use.

As these criteria are based on local approximations, it is important to check that they still give relevant results with a non infinitesimal length of propagation. A 2D study was

conducted in order to compare the direction given by X-FEM using the maximum hoop stress criterion and by calculating the values of the strain energy release rate when the direction of propagation is introduced manually. Figure 1 gives an example of the obtained results. The direction of propagation given by the local criteria corresponds to the maximum strain energy release rate propagation, as long as the length of propagation is small enough and adapted to the mesh size.

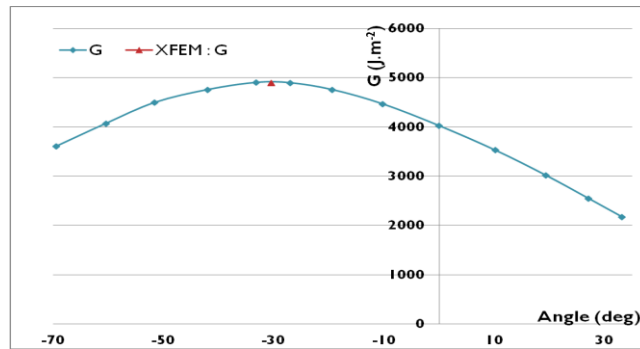


Figure 1. Verification of the accuracy of the direction of propagation.

However, the major drawback of these criteria is that they are based on a 2D plane strain theory. They have been extended to 3D due to a lack of theory describing 3D crack propagation. One can see that the misevaluation of the SIF in the crack front, combined with this lack of theory, can rapidly limit the accuracy of the simulated crack path.

Length of Propagation Criterion

Brittle crack propagation is based on Griffith's theory [8]. This theory aims at explaining when crack propagates. It introduces a critical strain energy release rate, G_c , that is a material parameter. When G is below G_c there is no propagation. When G reaches G_c there is propagation. It can be either stable or unstable.

The purpose of this paper is not to try and determine whether or not the crack will propagate. It is to determine the crack path in graphite bricks under several loadings, assuming at first glance that crack will propagate through the whole part. In this work the introduction of G_c in the criterion of propagation is a way to choose which points of the crack front are propagating, but not to determine if the crack propagates.

The criterion implemented states that the crack propagates an arbitrary constant distance for the points of the crack front where G is maximal (Griffith-adapted criterion). There is a flexibility in the number of points that propagate. The main reason is that if only one point propagates for each step of propagation it is possible to propagate only on one point whose G -value might have been misevaluated. Moreover, it takes a lot more computational time. This variability can affect crack path and a compromise has to be found.

The accuracy of the crack path is evaluated by analysing the compatibility with Mode I dominating and iso- G propagation. A preliminary study was conducted on a planar purely Mode I propagation, presented in Figure 2 (the plane represented is the

full cross-section of the body in which the crack propagates, and the different coloured lines are the representations of the crack front for different steps of propagation). Various initial crack shapes were tested. Though they were not the right ones (great dispersion of the values of G), the crack gradually propagates and the crack path becomes basically the same (linear crack front), reducing in each case the relative standard deviation. This study indicates that the initial crack shape is not influential when we use the Griffith-adapted criterion as crack naturally propagates to take the right shape. Several values of the length of propagation were tested: crack path is not significantly affected when the value is small compared to the dimensions of the part.

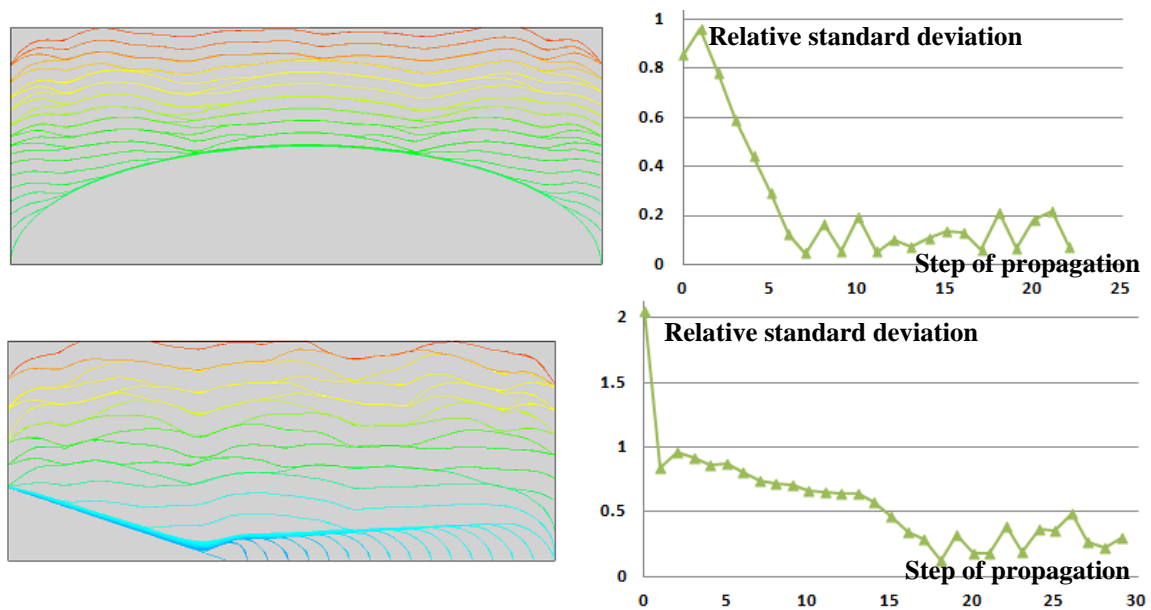


Figure 2. Evolution of the relative standard deviation with crack propagation.

TEST CASES BASED ON GRAPHITE BRICKS

Three test cases based on EDF Energy Nuclear Generation related reports are presented here. The gradual complexity of the crack path allows a study of the capabilities of the method to predict it and the evaluation of the validity and the robustness of the propagation criteria used.

Case 1: Simulation of Internal Loading on Slotted Sliced Bricks

Irradiation causes heterogeneous shrinkage of graphite, which leads to evolving internal stresses in the material. Un-irradiated bricks have been slotted and an experimental device applied a loading that simulates the effect of irradiation induced stresses (i.e. through wall bend stresses): the bore is submitted to compression while the external areas are in tension via a fixed end and a free end placed on both sides of the slot. Thus,

crack is likely to initiate in the external zones, and more particularly in the corners of the brick. Figure 3 presents the experimental device (3a), some experimental cracked bricks (3b) the numerical loading (3c) as well as one of the crack paths obtained (3d).

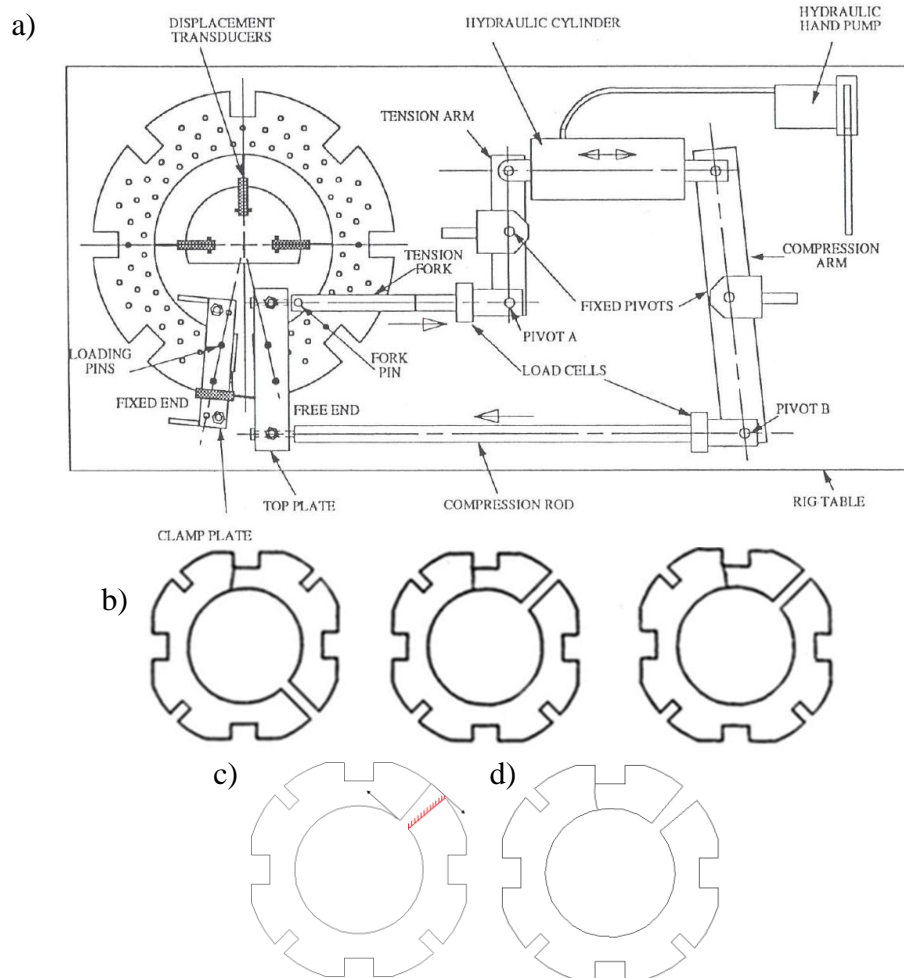


Figure 3. First test case: experimental and numerical results.

For this test, 2D results and 3D results are similar and close to the experimental radial crack path. 3D results are more difficult to obtain though, because of the influence of crack propagation criteria and of the initial crack shape. A relevant crack path can be obtained using the Griffith-adapted criterion on several different initial crack shapes. If we allow a lot of points to propagate at each step, the crack path is quite dependent on the initial crack path. When the number of points is reduced, it is possible to see that the crack propagates in accordance with the Mode I dominating and iso-G properties and that it does not significantly depend on the initial crack shape. Indeed, each crack propagates in order to give quite a similar path after a few steps of propagation. Though this criterion requires more computational time, it seems quite robust as it allows a change of geometry of the crack front when necessary.

Cases 2 and 3: External Loading on Sliced or Full-size Bricks

The AGR brick's geometry was designed to prevent cracks from appearing due to mutual interaction, even in case of unusual events such as earthquakes. Some experiments were conducted to establish the bricks' ultimate load bearing capacity, even if it was far above the anticipated loading in the AGR core.

Tests on sliced bricks (case 2) lead to a curved crack that propagates from a corner of the brick to the bore. Figure 4 presents the experimental device (4a), some experimental cracked bricks (4b), the numerical loading (4c) as well as one of the crack paths obtained (4d).

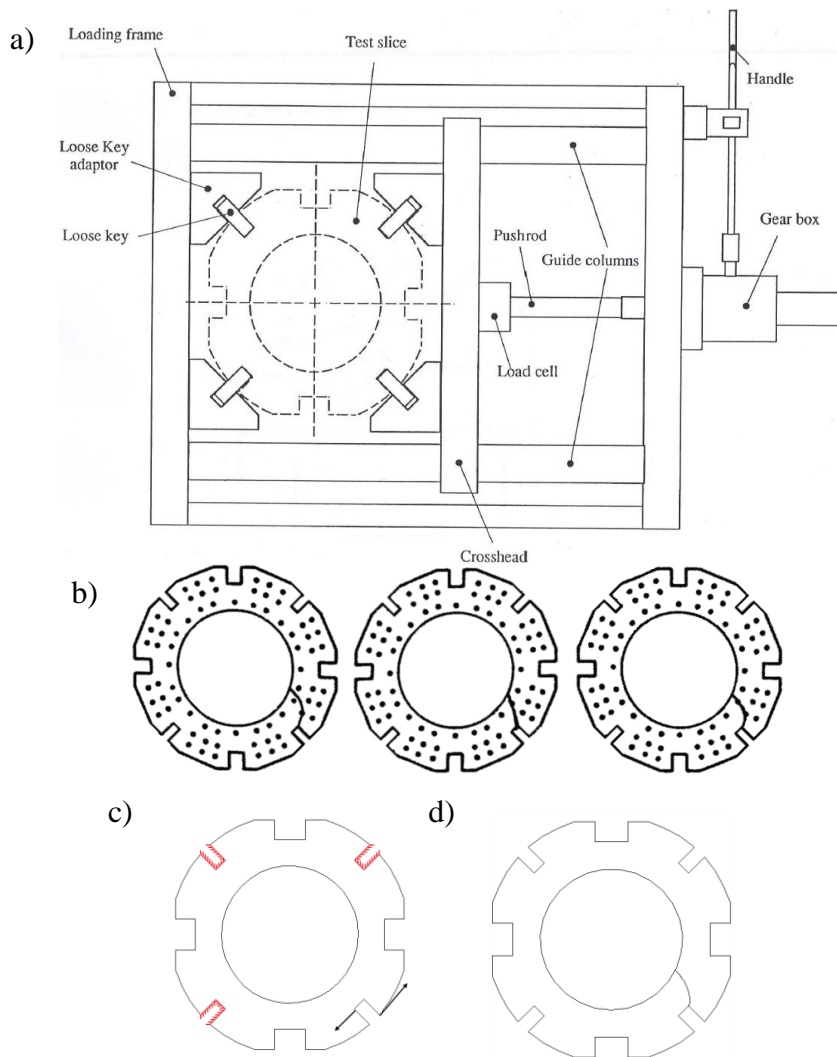


Figure 4. Second test case: experimental and numerical results.

For this test, 2D and 3D results are similar. The conclusions are the same as the one presented for the first test. However, the results are more dependent on the direction of the initial crack, which is also what can be observed in the experiments.

Tests on full-size bricks (case 3) lead to the more complex 3D crack path presented in Figure 5. This case is currently being studied. The results will help to determine whether or not the method used so far is sufficiently robust to predict such a crack path.



Figure 5. Crack path on the third test case.

CONCLUSION

The crack propagation criteria implemented in Code_Aster have proven to be quite robust and not mesh-dependent despite some problems encountered for the computational evaluation of the SIF and G in 3D. Propagation criteria were identified in order to be able to model brittle cracking propagation in 3D. Two test cases were conducted. For these two cases, crack paths obtained numerically appear to be close to experimental ones and in accordance with the Mode I dominating and the iso-G propagation. Even if the simulations were conducted in 3D, in order to test the ability of the code to perform such calculations, they can both be assimilated to 2D test cases. A third test case, which leads to a complex 3D crack path, is necessary to determine the validity domain of the modelling.

Acknowledgement: The authors gratefully acknowledge the support of EDF Energy Nuclear Generation and EDF R&D for this work. We thank Mr N. McLachlan, Dr A. Steer and Dr S. Géniaut for valuable input data and discussions.

REFERENCES

1. Bradford, M. R., Steer, A. G. (2008) *J. Nucl. Mater.* **381**, 137-144.
2. Melenk, J. Babuška, I. (1996) *Comput. Meths. Appl. Mech. Engrg* **139**, 289-314.
3. Moës, N., Gravouil, A., Belytschko, T. (2002) *Int. J. Numer. Meth. Engng* **53**, 2549-2568.
4. Hasebe, N., Nemat-Nasser, S., Keer, L.M. (1984) *Mech. Mater.* **3**, 147-156.
5. Pindra, N., Lazarus, V., Leblond, J.-B. (2008) *J. Mech. Phys. Solids* **56**, 1269-1295.
6. Géniaut, S., Massin, P., Moës, N., *11th International Conference on Fracture*, 20th-25th March 2005, Turin, Italy.
7. Decreuse, P.-Y. (2010). PhD Thesis, École Normale Supérieure de Cachan, France.
8. Lawn, B. (1993) *Fracture of Brittle Solids*, Cambridge University Press, 2nd Ed.